

Experimental and Numerical Investigation of Channeling Effects on Noise and Aerodynamic Performance of NACA 0012 Aerofoil in Wind Turbine Applications

Hussein K. Mohammad^{1,2}, S. M. Jalil^{3,4}, Arz Y. Qwam Alden⁴, Viktor Kilchyk⁵, Bade Shrestha¹

¹Western Michigan University, Mechanical and Aerospace Department

²University of Tikrit, College of Science, Physics Department

³Michigan State University, Department of Mechanical Engineering

⁴University of Anbar, Engineering College, Mechanical Department, Iraq

⁵Principle Aerothermal Engineer, Collins Aerospace

1 Hamilton Rd, Windsor Locks, CT

Abstract. *Wind power is considered one of the main sources of renewable energy in the market today. In this study, different sizes and directions of channels were created inside the NACA 0012 aerofoil, and the effect of these channels were investigated on aerodynamic noise and aerodynamic performance, experimentally and numerically. The results have shown several factors that could affect the aerodynamic noise such as flow velocity, angle of attack, and trailing edge blowing injection. The study also concluded an increase in drag coefficients and a decrease in lift coefficients for all channeled samples compared to the regular aerofoil. In contrast to the studies that showed improvements in the aerodynamic performance of supersonic channeled aerofoils, this study done under subsonic flow showed an increase in drag and decrease in lift.*

Key words. Wind noise, aerodynamic performance, channelling of NACA 0012 aerofoil.

1. INTRODUCTION

The world is looking for alternative and renewable sources of energy to combat the many environmental problems facing the world today from ubiquitous use of fossil fuels. Wind is one of the most promising sources of renewable energy moving forward as it is not only getting cheaper but also becoming more popular and resilient among energy sources. In fact, the global market of wind energy has nearly quadrupled in size in the last decade reaching 743 GW in 2020 [1].

However, the considerable expansion of wind turbine farms also creates problems arising from the operation of

farms including noise pollution, which mainly occur due to the formation of unsteady vortices on many scales behind the trailing edge of the wind turbines. It is annoying, especially for people and wildlife who live close to wind turbine farms.

During the last several decades, many researchers have tried to address this problem, especially as the number of farms have increased and moved closer to towns and cities to meet increasing demands for renewable energy [2-4].

Fite et al. [5] investigated, experimentally and numerically, the effect of trailing edge flow injection on fan noise and aerodynamic performance. Trailing edge blowing injection was used to reduce the wake momentum deficit of the fan blade. The study concluded that this technique reduced the overall sound power level by 2 dB with an average reduction of about 1.5 dB of broadband noise up to 20 kHz. Tone noise was reduced up to 6 dB in the 2 Blade Pass Frequency (BPF) tone at 6700 rpm. The results also indicated that there is no reduction in the aerodynamic performance. Some other studies focused on using porous material on the trailing edge as a possible approach to reduce the noise. Geyer et al. [6] investigated noise using several different porous materials with different chord wise extent. An open jet wind turbine was used with a set of microphones to collect the sound data including the aerodynamic performance measurement at the same time. The results concluded that porous trailing edge material reduces the noise with no loss in the aerodynamic performance as the aerofoil is non-porous except the trailing edge. In this study channels were injecting the flow at the trailing edge or near the trailing edge on one of the aerofoil sides, and this worked as a wake filling strategy.

Many studies also focused on improvement of the aerodynamic performance by decreasing the lift and drag

ratio by decreasing the drag (D) or increasing the lift (L) [7-12]. Gupta et al. and Ruffin et al [8, 9] investigated supersonic channels for an aerofoil at Mach 2.5. The results showed total drag decreased 30% for laminar flow and 20% for turbulent flow compared to the aerofoils without channels. They also investigated, in the two different studies, the supersonic channels of aerofoils. The first study focused on the sphere cone with a channel in the leading edge, at Mach 7, at the altitude of 20 km and angle of attack (AOA) of 5 degrees. The study showed an increase of 25.1% in L/D and revealed that when the channels get larger, the reduction in drag gets greater, up to 20% compared to a sphere cone without channel. In the second study, Gupta and Ruffin investigated the artificially blunted leading edge (ABLE) aerofoils at Mach 4 and at 12 km altitude; the results show 19% reduction in drag coefficient [10, 11].

Giles and Marshall [12] used a diamond shape supersonic channel design to improve the aerodynamic performance of a NACA 66-206 aerofoil. The numerical results showed an increase of 17.2% in lift to drag ratio for aerofoils at Mach 2.5, at 35000 ft altitude, and AOA of 6 degrees. The experimental results showed an increase of 9% lift to drag ratio under the same conditions.

In our study, NACA 0012, which is widely used in wind turbine blades [13,14], was employed to investigate the effect of channels on the aerodynamic noise and performance, experimentally and numerically. This study was done under different conditions at subsonic flow of 5, 10, and 15 m/s velocities and at three AOA (5, 10, 15 degrees). The study is the continuation of our paper, which is published in the ASME Journal, where we showed that the channeling has affected the reduction on the wind turbine noise [15]. The purpose of this current study is to investigate the effect of using channels inside aerofoils on the noise level as a noise reduction technique in wind turbines as well as the effect of these channels on aerodynamic performance including turbulence intensity.

2. EXPERIMENTAL SETUP AND METHODOLOGY

To conduct experiments for this research, a wind tunnel was added to the existing fluid dynamics laboratory. This wind tunnel can produce wind speeds of up to 65 mph and is enclosed in the newly built quiet chamber to make reliable noise measurement along with aerodynamic performance measurements. The quiet chamber is 10'x10'x9'. The walls, ceiling, and floor of the chamber are insulated by three layers of foam to isolate from exterior noises and vibrations. The exit of the wind tunnel is a circular diameter of 13 cm (Figure 1). On the other side, a hole of diameter 35 cm is created for the outflow.

In this study, NACA 0012 aerofoil was used as it is one of the most popular aerofoils in wind turbine applications. A total of twelve different aerofoil samples were created using SOLIDWORKS and built using 3D printing. The first sample was designed with no channels, while all other samples incorporated channels. The channels were created throughout the aerofoil starting from the leading edge along the length of the aerofoil chord. The channels

were designed with different sizes and different angles relative to the chord. Three different channel diameters were implemented in this study (0.05, 0.08, 0.1 inches), which were used in different angles between the channel and chord directions. The directions between the channels and chord were studied using four different directions (-1, 0, 2, and 3 degrees anticlockwise). At angle (-1) degree, two channel diameter sizes (0.05, 0.08 inches) were used. All samples were surface smooth finished using sandpapers of 20 different grit sizes (P60-P3000) to minimize aerodynamic noise. For each sample, three different AOAs (5, 10, and 15 degrees) and three different flow speeds (5, 10, and 15 m/s) were applied. And in Table (1), the terminology used to describe aerofoils are stated.

Aerodynamic noise was recorded using 4 different microphones and data was collected using the Smart Office application (Figure 1). The low frequency free field microphone with a frequency range of (0.13 to 20000 Hz) was used to measure the noise around the aerofoil and was located perpendicular to and 6 inches away from the trailing edge. The microphone was connected to the Smart Office application that could read and save the level of noise for all ranges of the interested frequencies.

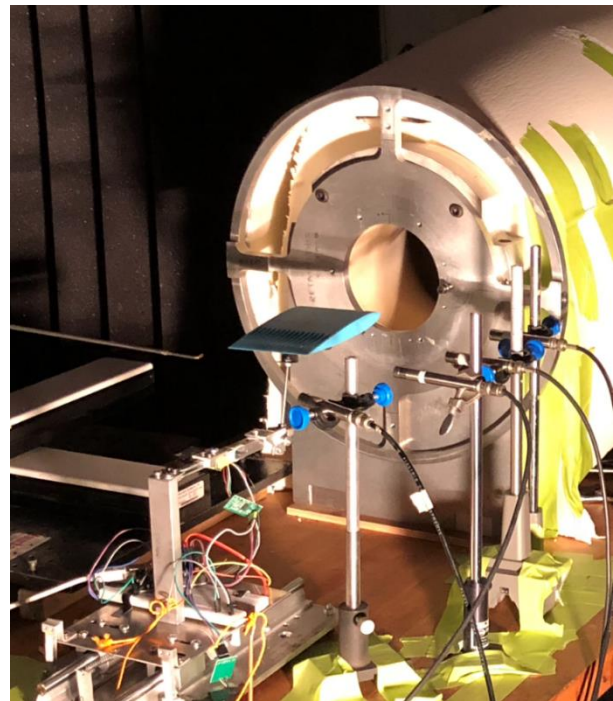


Figure 1. The microphones set up.

The ½-inch free field polarized microphone was used to measure infrasound at separate points simultaneously. Both were ICP Infrasound Microphone systems manufactured by PCB Piezotronics. The microphone system was composed of the microphone (Model: 377A07), preamplifier (Model: 426E01) and a low-frequency filter adapter (Model: 079A43). The complete system allowed for the measurement of noise down to 0.1 Hz. Before testing, the microphone was calibrated using a Larson Davis CAL200 Precision Acoustic Calibrator. The

CAL200 was set to a 94 dB noise source at 1kHz. The sensitivity was altered during calibration so that the output of the microphone was within 0.025% of the 94 dB source. This output was displayed numerically and graphically on a frequency spectrum within the m+p SmartOffice Dynamic Signal Acquisition and Analysis software.

Aerodynamic force measurements were carried out by a homemade force balance specially designed and built for this research using four load cells, two to measure the lift force (vertical forces) and two to measure the drag force (horizontal forces). The AOA was measured manually. Each load cell has four strain gauges that were connected to each other as a Wheatstone bridge. An aluminum alloy load cell, weighing sensor 500g capacity, was used to achieve the balance. The voltage from the load cells was read using Arduino which was connected to the computer to record the measured data (Figure 1).

regular NACA 0012 aerofoil with 5.5 inches as a chord length. Three channeled aerofoils of 3° inclination with the chord of diameters of 0.1, 0.08, and 0.05 inches were studied as shown in Figure (2) (d) for D=0.1 inch. The last channeled aerofoil was with 0.08 inch channel diameter and -1° inclination with the aerofoil chord. Figure (2) also illustrated the aerofoil's geometries and meshes at a 10° AOA. The far-field boundaries were set at 18 chords away from the leading edge in front, up, and down directions and 36 chords away in the back direction.

The mesh for each aerofoil were generated by using ANSYS Meshing 19.2 [16]. Five different meshes with several elements (46252, 136153, 198009, 360634, and 691094) were considered to test the mesh quality. To resolve the high intensity of the vorticity near the aerofoil wall, inflations of ten quadrilateral mesh layers were applied along the regular aerofoil and channeled aerofoil edges with a thickness of 1e-2 inch with 400 grid points along the aerofoil. To ensure that the simulations were mesh independent, four different parameters: drag

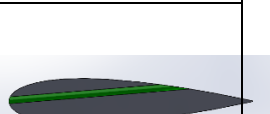
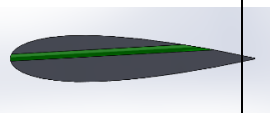
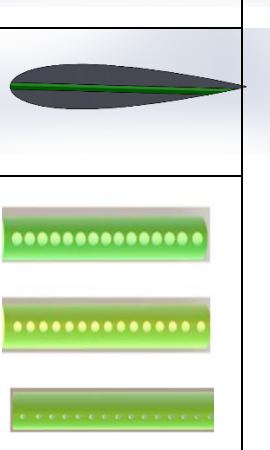
Sample name	Description	2 D section
Unchannel	Regular aerofoil with no channels	
A0	Sample has channels parallel to the chord of the aerofoil	
A3	Sample has channels with 3 degrees angle measured from the leading edge with respect to the chord in counterclockwise direction	
A2	Sample has channels with 2 degrees angle from the leading edge with respect to the chord in counterclockwise direction	
A-1	Sample has channels with 1 degree angle from the leading edge with respect to the chord in clockwise direction	
D0.1 D0.08 D0.05	Sample has 0.1 inch diameter size Sample has 0.08 inch diameter size Sample has 0.05 inch diameter size	

Table 1. The terminology used to describe airfoils.

3. NUMERICAL SIMULATION METHOD

For the numerical simulation, five different 2D models for NACA 0012 were considered. The primary aerofoil was a

coefficient (C_d), lift coefficient (C_l), wall shear stress τ_w , and dimensionless wall distance y^+ , were monitored in each mesh test. Along the aerofoil edges, y^+ was kept below one to capture the sharp change in velocity near the

wall [17]. As the error between mesh 4 and mesh 5 did not exceed 2%, mesh 4 was considered in the current simulations. For the channeled aerofoil, the same procedures were applied.

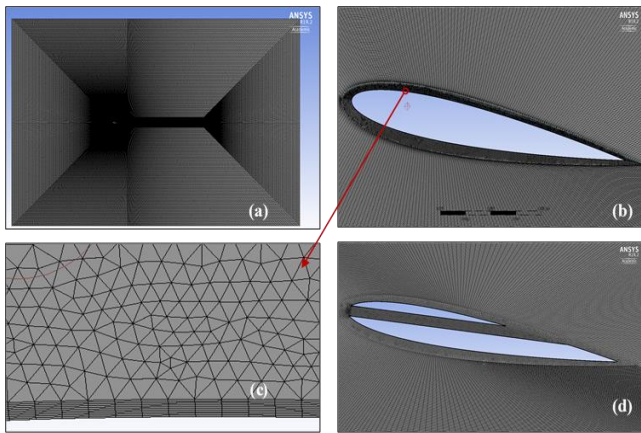


Figure 2. a) Regular aerofoil's entire domain. b) Aerofoil surface zoomed in. c) Aerofoil boundary layer zoomed in. d) Channeled aerofoil D=0.1 inch.

Turbulent modeling was carried out solving Navier-Stokes and energy equations by using a transient pressure-velocity coupling method of the SIMPLE scheme in FLUENT 19.2. Equations with pressure-based SST k- ω

turbulent model were employed for the closure of the Reynolds-Averaged Navier-Stokes (RANS) as below.

$$\frac{\partial \overline{u_i}}{\partial x_j} = 0 \quad (1)$$

$$\frac{\partial(\rho \overline{u_i})}{\partial t} + \frac{\partial(\rho \overline{u_i u_j})}{\partial x_j} = -\frac{\partial \overline{p}}{\partial x_i} + \frac{\partial}{\partial x_j} \left[\mu \left(\frac{\partial \overline{u_i}}{\partial x_j} + \frac{\partial \overline{u_j}}{\partial x_i} \right) \right] + \frac{\partial}{\partial x_j} (-\rho \overline{u_i' u_j'}) \quad (2)$$

Where ρ , p , μ represent the working fluid density, pressure, and dynamic viscosity. A scaled residual of 1×10^{-6} was used for all governing equations with 1×10^{-6} as a time step size to achieve a converged stable solution [17].

4 RESULTS AND DISCUSSION

The results of the investigation on wind turbine noise from various parameters such as wind velocities, AOA, channel sizes and dimeters are presented in this section. Figures (3) and (4) show the relation between sound pressure level (SPL) and wind velocity as examples for the unchannelled and A3 data sets. It can be seen from the figures that as the wind velocity gets larger the noise gets louder, as expected. Generally, increase in velocity of 5 m/s would increase noise by an average amount of 10 dB as shown in Table (3) for all cases.

X [Hz]	Unchannel	A3	A3	A3	A2	A2	A2	A-1	A-1	A0	A0	A0
		D0.08	D0.05	D0.1	D0.08	D0.05	D0.1	A0.08	D0.05	D0.08	D0.05	D0.1
31.5	43.89	42.59	44.13	44.67	48.23	46.97	46.00	45.80	47.44	45.49	46.64	46.68
63	49.56	47.60	46.03	44.32	48.75	53.06	46.23	44.63	49.60	44.70	45.65	50.42
125	45.81	43.30	47.84	42.91	46.87	51.40	44.80	51.17	48.95	47.78	49.83	47.48
250	28.43	35.04	45.57	37.80	41.55	46.84	36.99	53.55	52.96	51.07	54.13	50.71
500	27.93	33.52	38.97	33.64	39.58	52.21	36.38	46.06	47.31	42.94	47.25	42.26
1000	29.80	46.46	37.56	37.41	34.61	44.38	40.66	43.41	41.56	41.32	45.13	41.68
2000	15.59	37.99	27.36	35.33	21.52	36.28	30.60	32.99	35.68	36.30	37.85	36.03
4000	11.99	24.37	28.12	26.48	-1.10	26.66	25.07	27.81	28.91	25.21	27.37	28.48
8000	0.85	12.67	11.01	9.22	14.36	17.36	15.37	16.43	16.08	16.46	17.07	13.84
Overall (dBA)	51.91	51.86	52.49	49.71	53.36	58.04	51.29	56.90	56.95	54.63	57.24	55.64

Table 2. A-weighting adjustments for one octave center frequencies for all the samples at flow velocity 15 m/s.

Flow velocity	Unchannel	A3	A3	A3	A2	A2	A2	A-1	A-1	A0	A0	A0
		D0.08	D0.05	D0.1	D0.08	D0.05	D0.1	A0.08	D0.05	D0.08	D0.05	D0.1
5 m/s	32.88	32.21	30.21	32.10	32.39	34.63	33.45	35.89	34.71	34.38	38.47	34.06
10 m/s	41.2	40.5	42.2	40.7	41.1	47.6	40.7	46.4	46.2	44.7	46.7	44.9
15 m/s	51.91	51.86	52.49	49.71	53.36	58.04	51.29	56.90	56.95	54.63	57.24	55.64

Table 3. Overall SPL for all samples at flow velocities 5, 10, 15 m/s.

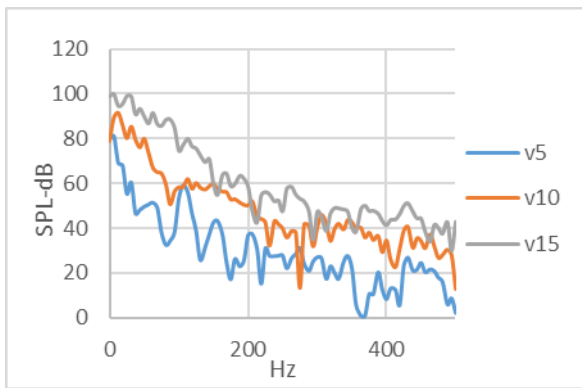


Figure 3. SPL vs. Freq. for Unchanneled sample for Velocities 5, 10, 15 m/s.

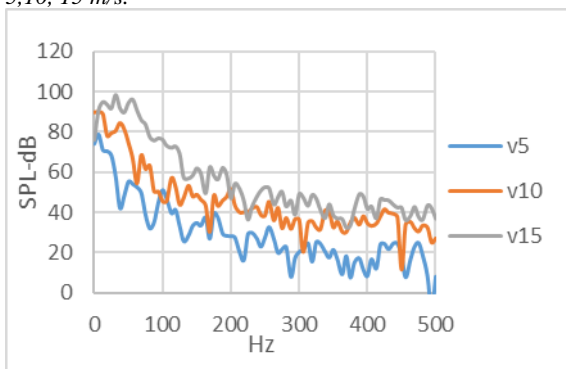


Figure 4. SPL vs. Freq. for A3 D0.1 sample for Velocities 5, 10, 15 m/s.

A-weighting adjustments for one octave center frequencies for all samples in wind velocity 15 m/s at 10 degrees of AOA were presented in Table (2) using overall SPL calculated by the following equation (3) [18, 19].

$$\text{Overall SPA (dBA)} = 10 * \log \left[\left(10 \right)^{\frac{S_1}{10}} + \left(10 \right)^{\frac{S_2}{10}} + \dots + \left(10 \right)^{\frac{S_n}{10}} \right] \quad (3)$$

Where: S1, S2 Sn are the SPL in A-weighting adjustments for one-octave center frequencies starting with 31.5 Hz to 8,000 Hz.

Similarly, the A-weighting adjustments for one-octave center frequencies for all samples in wind velocities 10 and 5 m/s at AOA 10° were calculated and the overall SPL are presented in Table (3) with 15 m/s wind speed data for comparison. For all wind speeds, the SPL noise level increased as the wind speed increased, as expected

The influence of AOA on the noise generation was also investigated and the results showed a direct relation between aerodynamic noise and the AOA of the samples.

Table (4) shows the overall SPL for the different samples at the wind speed of 10 m/s. For other wind speeds, the results were similar and not presented for brevity. Overall

AOA	Unchannel	A3 D0.08	A3 D0.05	A3 D0.1	A2 D0.08	A2 D0.05	A2 D0.1	A-1 A0.08	A-1 D0.05	A0 D0.08	A0 D0.05	A0 D0.1
5.00	40.11	40.11	40.52	38.91	39.72	44.56	40.32	45.18	44.94	43.87	42.77	42.99
10.00	41.16	40.51	42.21	40.74	41.07	47.63	40.69	46.40	46.18	44.72	46.65	44.94
15.00	43.26	41.88	47.11	43.06	47.36	49.86	40.85	51.18	46.02	50.76	47.82	47.06

Table 4. overall SPL for all samples with AOA 5, 10 15 at 10 m/s.

SPL was increased between (1-4 dBA) when AOA was increased from 5 to 10°, while there was an increase from (1-6 dBA) when AOA increased from 10 to 15°. Figure (5) shows the overall SPL for different AOA for all samples.

The influence of channel diameter and direction were investigated as well. According to Fite et al. [5] one technique in reducing overall SPL, broadband noise, and tone noise was to reduce the wake momentum deficit of the aerofoils. Hence, in this study, the channels were made to carry air flow from the leading edge all the way to the suction side in the aerofoils A3 and A2. In the aerofoil A-1, the channel carried air from the leading edge to the pressure side of the aerofoils. And in the aerofoil A-0 the air blows to the trailing edge of the aerofoils. These channels were injecting the flow at the trailing edge or near the trailing edge on one of the aerofoil sides, and worked as a wake filling strategy.

Figure (6) illustrates the noise spectrum for frequencies 0-600 Hz, which is the range where aerodynamic noises are mostly located. The figure shows the noise in sample D0.1 for three different directions, A3, A2, and A0. It could be noticed that the samples A2 and A3 produced less noise than the unchanneled sample. However, the sample A0 shows a higher level of noise than the unchanneled sample. It is found that the diameter of 0.05 inches (D0.05), generated a high level of noise compared to the unchanneled sample for all angles except for sample A3. The samples with a diameter of 0.08 inches (D0.08) show similar behavior as samples with D0.05. In conclusion, the sample that produced the least amount of noise, regardless of channel size, was the channel with a 3° inclination angle (the A3 case). The flow in this sample went to the suction surface where the most turbulence happened. The flow in sample A3 helped the wake momentum deficit and reduced the pressure fluctuation, eventually reducing the noise generated by the fluctuations.

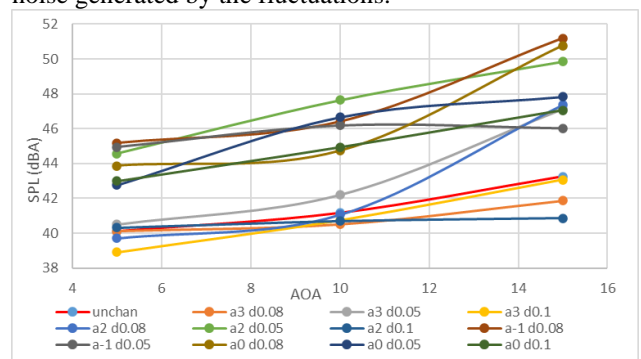


Figure 5. Overall SPL vs. AOA for all samples.

	Cd			Cl		
	AOA	AOA	AOA	AOA	AOA	AOA
	5	10	15	5	10	15
Unchannel	0.045	0.069	0.085	0.305	0.574	0.708
A3 D0.08	0.048	0.071	0.091	0.275	0.520	0.631
A3 D0.05	0.047	0.070	0.088	0.295	0.573	0.694
A3 D0.1	0.051	0.071	0.092	0.275	0.515	0.625
A2 D0.08	0.054	0.076	0.096	0.299	0.495	0.627
A2 D0.05	0.062	0.083	0.104	0.264	0.495	0.635
A2 D0.1	0.065	0.083	0.106	0.255	0.465	0.595
A-1 D0.08	0.062	0.085	0.108	0.295	0.497	0.615
A-1 D0.05	0.063	0.081	0.105	0.312	0.515	0.625
A0 D0.08	0.063	0.083	0.106	0.298	0.545	0.655
A0 D0.05	0.059	0.078	0.102	0.305	0.555	0.673
A0 D0.1	0.065	0.085	0.109	0.298	0.535	0.635

Table 5. Experimental results of lift and drag coefficients for all samples at flow velocity 5 m/s.

Figure (7) presents the noise spectrum for frequencies 0-600 Hz for different channel sizes at the wind speed of 10 m/s as an example. The influence of size of channels on the aerodynamic noise were studied for all different samples. The results showed that the samples with (D0.1) were quieter than the samples (D0.08) and the samples (D0.05) (Table 2, 3 and 4). As a conclusion, the size of channels had significant influence on the aerodynamic noise, and as the channel size gets smaller, the noise gets louder

Simultaneous with the noise measurement, the aerodynamic forces were also recorded during the experimentation to investigate the aerodynamic performance of the aerofoils in all conditions and wind speeds employed. The results showed similarity of the effects of channels on aerodynamic forces for different velocities. Therefore, the results of the velocity (5 m/s) were displayed. Table (5) shows the drag coefficients and lift coefficients for the 12 different samples for AOA of 5°, 10°, and 15°.

Figure (8) shows the experimental results of Cl/Cd for different samples under different AOA as an example. The presence of channels for all samples reduced the ratio Cl/Cd in comparison to the unchannelled case. However, the loss is minimal for the A3 cases.

An increases in channel size lead to a decrease in efficiency, making the relation between channel size and efficiency inverse in nature.

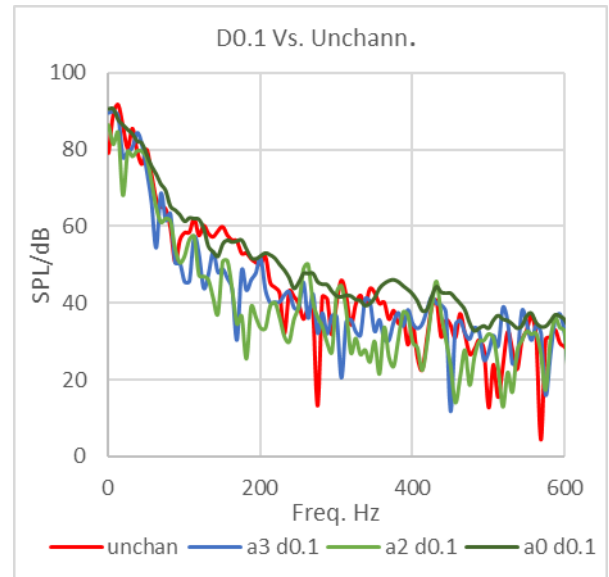


Figure 6. SPL vs. Freq. for D0.1 sample for different angles at 10 m/s velocity.

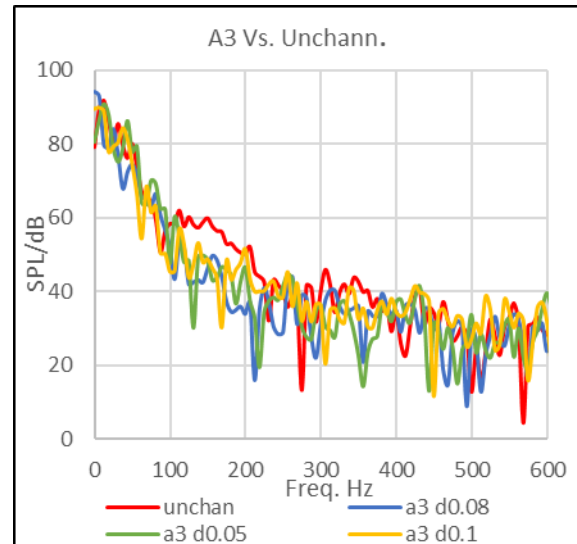


Figure 7. SPL vs. Freq. for A3 sample for different diameters at 10 m/s velocity.

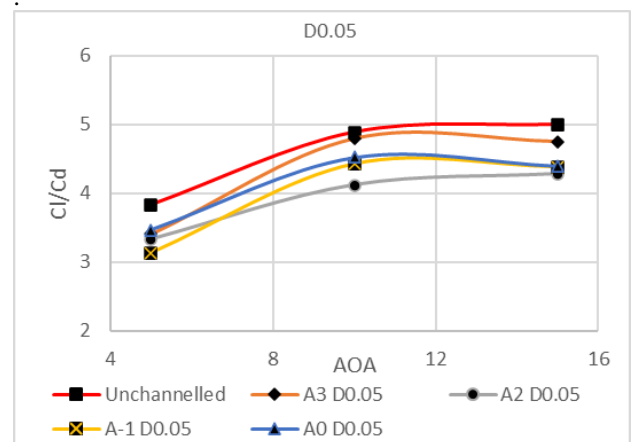


Figure 8. Cl/Cd vs. AOA for D0.05 sample for different angles.

As seen in table (5), drag coefficient increased between (0 - 2 %) in sample A3 D0.05, the best among all samples. However, for the two samples A-1 D0.08 and

A0 D0.1, the drag coefficient increased the most (12 - 23%), the worst among all samples. In the lift section of the table, the lift coefficient for sample A0 D0.05 decreased between (0 - 2 %) in comparison to the unchanneled aerofoil, the best among the samples. However, for the sample A2 D0.1, the lift coefficient decreased the most (12 - 15%), the worst among all samples.

Mainly, drag can be classified into many categories: skin friction, form, interference, lift induced, and wave. In supersonic flow, the pressure drag, especially wave drag, is dominant. Hence, channels in the aerofoil will help to reduce the pressure in front of the leading edge causing a reduction in wave drag. The reduction in wave drag outweighs the increase in skin friction drag that results from an increased wetted area due to the channels. As a result of using channels in supersonic flow, the ratio (L/D) will increase, improving the aerodynamic performance [9][12].

In our study with subsonic flow, the skin friction drag (viscous drag) is dominant. The drag gets larger with the channels as the channels give more skin friction area (wetted area) compared to the aerofoil without channels causing the ratio (L/D) to decrease reducing the aerodynamic performance for the employed aerofoil. In principle, it can be resolved using different aerofoils and designs.

In conclusion, the channels have been shown to reduce the wind turbine noise as well as reduce the aerodynamic performance. The channels have different influences on aerodynamic performance depending on the channel size or channel direction. From all 12 samples that have been studied, the sample A3 showed the best reduction of noise with an efficiency loss of less than 2%.

5. COMPARISON BETWEEN EXPERIMENTAL AND NUMERICAL RESULTS

Table (6) presents the experimental results and the numerical results of the overall noise for four samples: unchanneled, A3 D0.1, A3 D0.08, and A3 D0.05 at velocity 15 m/s. The experimental results were close to the numerical results for the samples unchanneled and A3 D0.08. The error in these two samples are 4% and 7% , respectively. However, there is a noticeable difference in results for samples A3 D0.1 and A3 D0.05 within 15% and 28% errors.

Flow velocity 15 m/s	Unchannel	A3 D0.08	A3 D0.05	A3 D0.1
Experimental	51.91	51.86	52.49	49.71
Simulation	49.5	48.1	44.5	35.6
Error	0.04	0.07	0.15	0.28

Table 6. Experimental and numerical results for overall noise.

Similarly, the comparison between experimental and numerical results of lift and drag coefficients were carried

out for some samples as shown in table (7). The experimental results were higher for some Cd and generally lower for Cl, as expected. This is because in 2D simulation the 3D surface smoothness, limitation on measurement accuracy, and other factors which are present during experimentation are not considered. However, the error can generally be considered within the experimental errors.

Cases	AO A	V	Cd		Cl	
			Exp	Num	Exp	Num
unchanneled	10°	5	0.09	0.07	0.47	0.58
	10°	15	0.054	0.03	0.64	0.89
A3 D0.05	10°	15	0.055	0.061	0.63	0.73
A3 D0.1	10°	5	0.09	0.019	0.43	0.054
	10°	10	0.071	0.082	0.52	0.589
	10°	15	0.063	0.078	0.57	0.58
	5°	15	0.047	0.03	0.315	0.317
A-1 D0.08	10°	15	0.075	0.23	0.58	2.06
A3 D0.08	10°	15	0.058	0.075	0.61	0.61

Table 7. Experimental and numerical results of lift and drag coefficients for some samples.

6. CONCLUSION

Wind power is one of the main growing sources of renewable energy on the market today. The aerodynamic noise emitted from wind turbines is one drawback that needs to be addressed. In this study, channels were created inside the aerofoils to inject the flow from leading edge to trailing edge to reduce the wake momentum deficit. The results showed improvements in aerodynamic noise in some samples. The study also concluded that several factors could affect the aerodynamic noise such as flow velocity, angle of attack, and trailing edge blowing injection.

Past studies of aerodynamic performance have shown an increase in lift and a decrease in drag as an effect of channels on aerodynamic performance of aerofoil in supersonic flow. In this study of aerofoil in subsonic flow, different sizes and directions of channels were created inside NACA 0012 aerofoil and have been tested under subsonic flow conditions. The effects of these channels were investigated on both aerodynamic noise and aerodynamic performance, experimentally and numerically. The channels were made at three different diameter sizes (0.05, 0.08, and 0.1 inches) and with four angles (-1 °, 0 °, 2 °, and 3°) with respect to the chord. The results showed an increase in drag coefficients and a

decrease in lift coefficients for all channeled samples compared to the regular unchanneled aerofoil.

In contrast to the past studies that showed improvements in the aerodynamic performance of supersonic channeled aerofoils because in supersonic flow the pressure drag was dominant, the channels decreased this drag and eventually the channels increased the ratio (L/D). In this study of subsonic flow, the skin friction drag (viscous drag) is dominant and the drag increased with the channels as the channels increased the skin friction area (wetted area) compared to the aerofoil without channels. The study showed, with several samples, improvement in noise reduction particularly in the case of A3 aerofoil. Additionally, it showed a reduction in aerodynamic performance, in some samples the reduction of aerodynamic performance did not exceed 1-2 %.

ACKNOWLEDGEMENTS

This research was supported by Department of Mechanical & Aerospace Engineering, Western Michigan University. The scholarship was provided by the Iraqi government.

References

- [1] Council, G. W. E. (2021). GWEC| global wind report 2021. *Global Wind Energy Council: Brussels, Belgium*.
- [2] Erkan, O., Özkan, M., Karakoç, T. H., Garrett, S. J., & Thomas, P. J. (2020). Investigation of aerodynamic performance characteristics of a wind-turbine-blade profile using the finite-volume method. *Renewable Energy*, *161*, 1359-1367.
- [3] Chen, Z., Wang, X., Guo, Y., & Kang, S. (2021). Numerical analysis of unsteady aerodynamic performance of floating offshore wind turbine under platform surge and pitch motions. *Renewable Energy*, *163*, 1849-1870.
- [4] Hongpeng, L., Yu, W., Rujing, Y., Peng, X., & Qing, W. (2020). Influence of the modification of asymmetric trailing-edge thickness on the aerodynamic performance of a wind turbine aerofoil. *Renewable Energy*, *147*, 1623-1631.
- [5] Fite, E., Woodward, R., & Podboy, G. (2006, June). Effect of trailing edge flow injection on fan noise and aerodynamic performance. In *3rd AIAA flow control conference* (p. 2844).
- [6] Geyer, T. F., & Sarradj, E. (2014). Trailing edge noise of partially porous aerofoils. In *20th AIAA/CEAS aeroacoustics conference* (p. 3039).
- [7] Young, T. M. (2017). *Performance of the Jet Transport Airplane: Analysis Methods, Flight Operations, and Regulations*. John Wiley & Sons.
- [8] Gupta, A., Ruffin, S., Gupta, A., & Ruffin, S. (1997, January). Aerothermodynamic design of supersonic channel aerofoils for drag reduction. In *1997 World Aviation Congress* (p. 5572).
- [9] Ruffin, S. M., Gupta, A., & Marshall, D. (2000). Supersonic channel aerofoils for reduced drag. *AIAA journal*, *38*(3), 480-486.
- [10] Gupta, A., Ruffin, S. M., Newfield, M. E., & Yates, L. (2000). Aerothermodynamic performance enhancement of sphere-cones using the artificially blunted leading-edge concept. *Journal of Spacecraft and Rockets*, *37*(2), 235-241.
- [11] Gupta, A., & Ruffin, S. M. (1999). Optimal artificially blunted leading-edge aerofoils for enhanced aerothermodynamic performance. *Journal of spacecraft and rockets*, *36*(4), 499-506.
- [12] Giles, D., & Marshall, D. (2008). Aerodynamic Performance Enhancement of a NACA 66-206 Aerofoil Using Supersonic Channel Aerofoil Design. In *46th AIAA Aerospace Sciences Meeting and Exhibit* (p. 300).
- [13] Michos, A., Bergeles, G., & Athanassiadis, N. (1983). Aerodynamic characteristics of NACA 0012 aerofoil in relation to wind generators. *Wind Engineering*, 247-262.
- [14] Oukassou, K., El Mouhsine, S., El Hajjaji, A., & Kharbouch, B. (2019). Comparison of the power, lift and drag coefficients of wind turbine blade from aerodynamics characteristics of Naca0012 and Naca2412. *Procedia Manufacturing*, *32*, 983-990.
- [15] Mohammad, H. K., Ibraheem, L., Kilchyk, V., & Shrestha, B. (2021). Experimental Investigation of Turbulence Effects on Aerodynamics Noise of Channeled NACA 0012 Aerofoil. *Journal of Solar Energy Engineering*, *143*(6).
- [16] Fluent, A. N. S. Y. S. (2011). Ansys fluent theory guide. *Ansys Inc., USA*, 15317, 724-746.
- [17] Jalil, S. M. (2020). Numerical characterization of viscous heat dissipation rate in oscillatory air flow. *Journal of Heat Transfer*, *142*(1), 011801.
- [18] Lord, H. W., Gatley, W. S., & Evensen, H. A. (1980). *Noise control for engineers*. McGraw-Hill Companies.
- [19] Bies, D. A., Hansen, C. H., & Howard, C. Q. (2017). *Engineering noise control*. CRC Press.